كلية الهندسة بشبرا
FACULTY OF ENGINEERING AT SHOUBRA
ERJ
PRINT ISSN 3009-6049
ONLINE ISSN 3009-6022

ENGINEERING RESEARCH JOURNAL (ERJ)
Volume (53),Issue (1)
January 2024, pp:181-188
https://erjsh.journals.ekb.eg

INVESTIGATING TIG ARC WELDMENTS FOR AUSTENITIC STAINLESS STEEL 304 AND 304L: A MECHANICAL AND METALLURGICAL ANALYSIS

Rasha Afify[1], Hamed A. Abdel-Aleem[2], Mohammed Gamil[1,*]

[1] Department of Mechanical Engineering, Faculty of Engineering at Shoubra, Benha University, Cairo 11629, Egypt.
[2]Welding Technology and NDT Department, Central Metallurgical Research and Development Institute (CMRDI), Cairo 11422, Egypt
**Corresponding author*

E-mail address: remasm7md33@gmail.com, hamedaa@gmail.com, mohammed.gamil@feng.bu.edu.eg

Abstract: In this study, the mechanical properties and microstructural characteristics of welded joints made from stainless steels 304 and 304L were investigated with respect to the applied TIG welding parameters, including the filler type, and applied current. Two different filler electrodes (ER304 and ER309) were used, and two distinct currents (70 and 80 A) were applied during the welding process. The dissimilar metals being joined had a thickness of 2 mm. The welded joints were evaluated using X-Ray radiography examination, tensile strength testing, microhardness testing, and microstructure investigation under all proposed welding conditions. The examination results revealed that all welding passes were continuous and free of internal defects, except for the specimens welded with ER309 at 70 A. The Specimen welded with ER304 at 80 A demonstrated the highest average maximum tensile strength (UTS) of 692 MPa, while the Specimen welded with ER309 at 70 A had the lowest average UTS of 670 MPa. It was observed that welding with 80 A resulted in higher mechanical properties than welding with 70 A. The microhardness of the base metal (BM), heat-affected zone (HAZ), and weld zone (WZ) was measured for all welding conditions. A dendritic structure was formed at the WZ of the welded joints, with ferrite and austenite homogeneously distributed throughout. Consequently, based on the excellent properties obtained, ER304 at 80 A is recommended for high-tech industrial applications.

Keywords: Austenitic stainless steel, TIG welding, Welding parameters, Mechanical performance.

1. Introduction

Austenitic stainless-steel grades are highly versatile and find applications in various engineering fields such as shipbuilding, machinery, heat exchangers, aerospace, and marine applications due to their excellent properties like high strength, toughness, and corrosion resistance [1, 2]. These grades are mainly composed of iron, chromium, and nickel, where the chromium content contributes to its high corrosion resistance, whereas the nickel content enhances its ductility and toughness. Among the various austenitic stainless-steel grades, AISI 304 and AISI 304L are of particular interest due to their industrial significance and wide usage [3].

Joining Austenitic stainless-steel grades (AISI 304, AISI 304L) can be accomplished using various welding techniques including TIG, MIG, laser beam, arc welding, and friction welding. TIG welding is widely preferred for its high-quality welds without defects and ability to create a smooth surface free from contamination [4, 5]. However, due to the unique chemical composition of these grades, issues such as joint embrittlement, hot cracks, stress corrosion cracking, and intergranular corrosion can arise. Therefore, optimizing welding parameters such as current, gas flow rate, and electrode diameter is crucial [6].

Numerous studies have explored the impact of welding parameters on the mechanical properties of TIG welded stainless steel. Manabendra, for example, found that the ideal welding conditions for achieving the highest UTS were 90 A, 12 m/min, and 3.2 mm for current, gas flow, and filler rod diameter, respectively [7]. In addition [5], investigated the impact of welding current on both the mechanical and microstructural properties of stainless steel 304. Their findings indicated that a welding current of 170 A resulted in the highest ultimate tensile strength, and that the hardness values of the welded specimens were greater than those of the base material. Additionally [8], proposed a double shielded TIG method to enhance weld penetration in comparison to the conventional TIG welding technique for AZG0Cr13Ni5Mo martensitic stainless steel. They investigated the effect of welding speed and current in the range of 1.5 mm/s to 5 mm/s and 100 A to 240 A, respectively.

In a study by [9], it was demonstrated that high welding current leads to lower hardness values in the weld zone. Conversely, increasing the welding speed has a positive impact on hardness values. Additionally, the bead width and depth of penetration were found to be directly proportional to the applied current and gas pressure, and inversely proportional to the welding speed. Moreover, [10] investigated the impact of TIG welding on Austenitic stainless steels, specifically type 304 and 304L, as materials

for pressure vessels. The study examined the tensile strength of the welded specimens before and after welding, as well as the microstructure of the materials. Furthermore, [11] conducted a study on TIG welded joints of 304 stainless steel, analyzing tensile tests, microstructure, and hardness measurements. They found that compared to the base metal, the hardness value of the welding zone decreased while the heat affected zone (HAZ) had a higher hardness value. The HAZ had a coarse-grained structure, which negatively affected the HAZ hardness.

[12] conducted a study to examine the impact of primary process input parameters on the weld geometry, mechanical properties, and metallurgical characteristics of weldments made from 3.8-mm-thick plates of austenitic stainless-steel type 304L using TIG welding with pulsed and non-pulsed current processes. Based on the microstructure analysis, it was found that the specimens welded with high pulse frequency current had a finer grain size, increased residual ferrite, and lacked columnar grains. This welding technique had a notable impact on the tensile strength and microhardness of the weldments, which differed from the results obtained with continuous current welding. Moreover, [13] reported that the microscopic examination of similar metal joints revealed a fine grain structure of small size in the weld zone, while the base metal had a larger grain structure. This suggests that there was a fine rearrangement of grains in the weld zone.

A literature review revealed that no published studies have investigated the impact of different filler electrodes and current variation on the microstructure and mechanical behavior of dissimilar metal welding between AISI 304 and AISI 304L stainless steel. Therefore, the objective of this research is to investigate the optimal process parameter values for TIG welding, including the type of filler electrode and applied current, to enhance the microstructure and mechanical properties of the welded joint**.**

2. MATERIAL AND METHODS

To investigate the weldability of two welded materials and the type of filler electrode, it is important to study the chemical compositions of the welded materials. **Table 1** and **Table 2** show the chemical compositions of the welded metals and the consumed electrode, respectively. **Table 1** displays the chemical composition of the two base metals to be welded using TIG, which are stainless steels 304 and 304L. Stainless steel 304L has a lower carbon content than stainless steel 304, and both alloys have a minimum of 18% chromium and 8% nickel. Additionally, both alloys have a maximum of 1.65 wt.% manganese, 0.0288 wt.% phosphorus, and 0.0046 wt.% sulfur. The lower carbon content in stainless steel 304L reduces the likelihood of carbide precipitation during TIG welding, resulting in higher corrosion resistance and suitability for use in severe corrosion environments. Moreover, the low carbon content contributes to a lower carbon equivalent, which indicates good weldability [14].

Table 2 shows the chemical composition of the two proposed consumable electrodes ER304 and ER309 for welding AISI 304 and AISI 304L stainless steel. ER309 has a higher percentage of alloying elements than ER304, which is expected to have an impact on the metallurgical and mechanical properties of the resulting welded joints. Moreover, **Table 3** presents the tensile properties of the consumed electrodes used for welding the two base metals. It is worth noting that ER309 has a higher yield strength of 400 MPa compared to ER304's yield strength of 265 MPa. However, ER309 has lower UTS, and elongation compared to ER304.

To create a butt joint using TIG welding, we utilized stainless steel welding specimens that were 2 mm thick, 200 mm long along the welding line, and 100 mm wide as shown in **Fig. 1**. Following the welding process, we conducted an X-ray radiography examination (YXLON International AS, SMART 583) on the welded specimens to confirm the absence of any welding defects within the welding passes. Tensile specimens were then cut perpendicular to the welding passes using a wire cutting machine, according to ASTM E8 standards [15]. To validate the results, we cut three tensile welding specimens at each welding condition. A visual representation of the cut tensile test specimens for the weld joints of stainless steels 304 and 304L is typically provided in a schematic illustration as depicted in **Fig. 2**. Uniaxial tensile testing was performed by using a hydraulic universal testing machine (UH-F1000KNI SHIMADZU, Tokyo, Japan) at a quasi-static strain rate of 10^{-3} s^{-1} at room temperature.

Table 1 Chemical composition of the base metals, stainless steels 304 and 304L (wt.%)

Material	C	Si	Mn	Cr	Ni	Mo	P	S	Fe
stainless steels 304	0.0238	0.501	1.65	18.70	8.00	0.0098	0.0215	0.0034	Balance
stainless steels 304L	0.0085	0.335	1.18	18.60	8.50	0.302	0.0288	0.0046	Balance

Table 2 Chemical composition of the consumable electrodes (wt.%)

Electrode Type	C	Si	Mn	Cr	Ni	Mo	Cu	P	S	Fe
ER304	0.02	0.5	1.65	18.7	8	0.01	0.002	0.022	0.003	Balance
ER309	0.06	0.4	1.8	23.5	13	0.25	0.2	0.018	0.015	Balance

Table 3 Tensile properties of the consumed electrodes

Material	Yield Strength (MPa)	Ultimate strength (MPa)	Elongation (%)
ER304	265	650	55
ER309	400	600	47

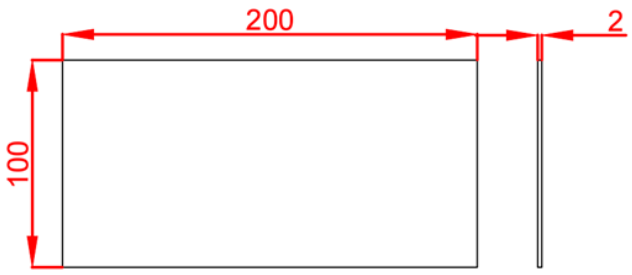

Fig. 1 Specimen dimension (all dimension in mm)

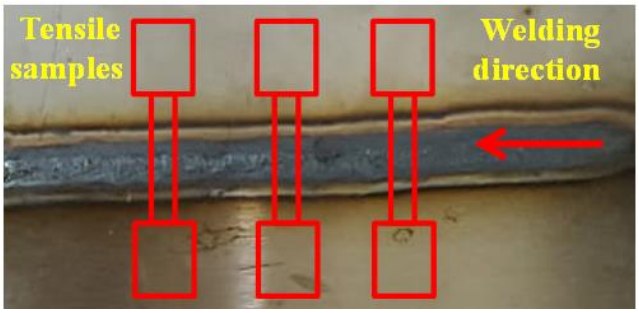

Fig. 2 Schematic illustration for the cut tensile test specimens for the welding joints of stainless steels 304 and 304L

The Vickers hardness test (HV) was performed on the base metal (BM), heat affected zone (HAZ), and weld metal (WM) at room temperature, according to ASTM E92-82 [16]. A diamond indenter was used with a 10 Kgf load and a 15-second dwell time. To ensure clear visualization of the results within each of these three areas, three measurements were taken within each zone. The purpose of the microhardness tests is to determine the hardness of the material in each of these regions, which can provide insights into the microstructure and mechanical properties of the welded joint.

To investigate the microstructure of the welded joints, appropriate specimens were cut at each welding condition. The specimens were mounted, ground, and polished before being rinsed with water, cleaned with acetone, and dried using a hand drier. The next step was to etch the specimens using a mixture consisting of 2.125 g of ferric chloride, 0.6 g of cupric chloride, 31 ml of alcohol, 31 ml of hydrochloric acid, and 1.5 ml of nitric acid. This etching process helps to reveal the microstructure of the material [17].

Finally, the microstructures of the different zones (i.e., PM, HAZ, and WM) were observed using an optical microscope (Olympus PMG3, Waltham, MA, USA). This technique allows for the visualization of the microstructure features such as grain size, grain boundaries, and the presence of any defects or inclusions. By examining the microstructure of the welded joints, it is possible to gain insights into the metallurgical changes that occur during the welding process and their impact on the mechanical properties of the joint.

In **Table 4**, we present the welding parameters that were utilized in this study. These parameters were selected based on a literature survey and several experimental trials that demonstrated higher welding accuracy without any defects. Two different welding currents (70 A and 80 A) were applied, along with two different filler electrodes. The welding times were recorded, and the welding speeds were subsequently calculated. Furthermore, the heat input (Q) for each welding process was calculated using Equation (1).

Where V represents voltage, I represents current, v represents welding speed, and k represents the coefficient of thermal efficiency of the specific welding process for TIG (0.6).

Table 4 Welding conditions and process parameters for TIG welding

Experiment No.	Filler type	Current (A)	Voltage (V)	Time (sec)	Speed (mm/min)	Efficiency (%)	Heat Input (J/mm)
1	ER309	70	10.5	1.4	142.8	60	185
2	ER309	80	11	1.2	166.6	60	190
3	ER304	70	10.5	2	100	60	265
4	ER304	80	11	1.55	129	60	246

3. RESULTS AND DISCUSSION

Figure 3 illustrates the appearance of the weld bead for the four welding conditions listed in **Table 4**. The welding passes are continuous and free of any visible welding defects, such as cracks, porosity, or incomplete fusion. The welding surface is smooth and clean, indicating a high-quality weld**.** The HAZ and WZ are also clearly visible due to the colour difference resulting from the welding process. Notably, specimens welded at 80 A (specimens 2 and 4) exhibit a smooth and uniform appearance without any visible imperfections. Conversely, specimens welded at 70 A have a visualized rough surface. Consequently, it is recommended to weld with 80 A to attain a good welding surface appearance. Furthermore, it is worth noting that the heat-affected zone (HAZ) and the root of the weld appear to be wider on specimens 2 and 4 compared to specimens 1 and 3. This is likely due to the higher heat input resulting from the use of a higher welding current (80 A), which led to more heat accumulation in the base metal as listed in **Table 4**. The wider HAZ and root of the weld in specimens 2 and 4 may have implications for the mechanical properties of the weld, such as strength and toughness, and should be taken into consideration when evaluating the suitability of the weld for its intended application.

An X-ray radiography examination was conducted as a non-destructive testing technique to detect any internal welding defects or abnormalities in the welded Specimens, as depicted in **Fig. 4**. Interestingly, the welding passes were found to be continuous without any internal defects such as internal cracks, porosity, or incomplete fusion for

experiments 1, 2, and 3, as shown in Fig. 3 (b, c, d). However, incomplete fusion was observed in **Fig. 4 (a)**, which represents experiment number one. The incomplete fusion results from the low applied current (70 A) and the high welding speed (1.4 Sec).

Figure 5 presents the tensile test specimens machined by the wire cut process. The welding passes are within the gauge length of the welded specimens **Table 4** presents the tensile test results of the welded specimens. The tabulated tensile test results represent the average of three specimens at each welding condition to ensure the repeatability of the results.

Table 5 provides information on the yield strength, UTS, and elongation of the two base metals welded in this study, namely stainless steel 304 and stainless steel 304L. The table shows that stainless steel 304 has a higher UTS value of 650 MPa but a lower yield strength of 265 MPa compared to stainless steel 304L, which has a UTS value of 620 MPa and a yield strength of 310 MPa. This suggests that stainless steel 304L has higher strength and is more resistant to plastic deformation compared to stainless steel 304. The elongation values for both materials are also provided in the table, indicating the ability of the materials to deform before fracture.

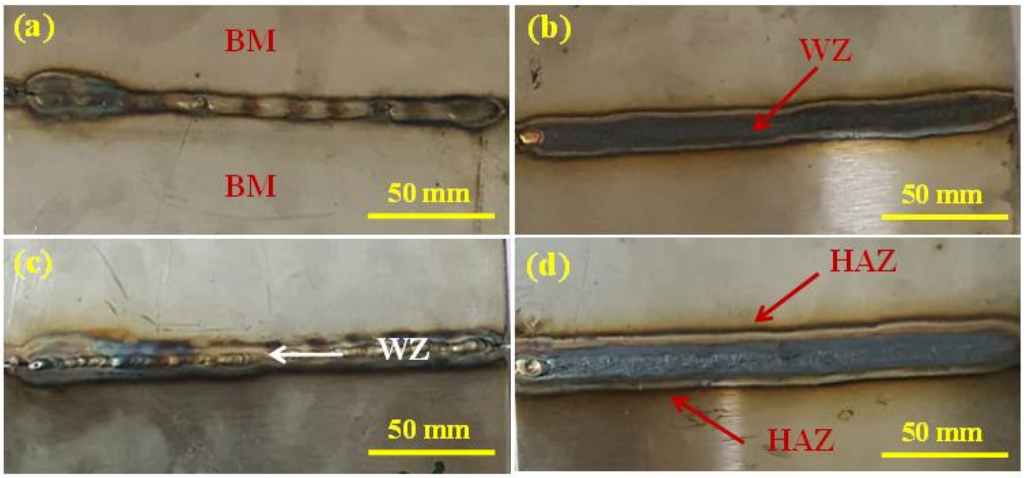

Fig. 3 The welded joints between stainless steels 304 and 304L at different welding conditions (a) ER309 and 70 A (b) ER309 and 80 A (c) ER304 and 70 A (d) ER304 and 80 A

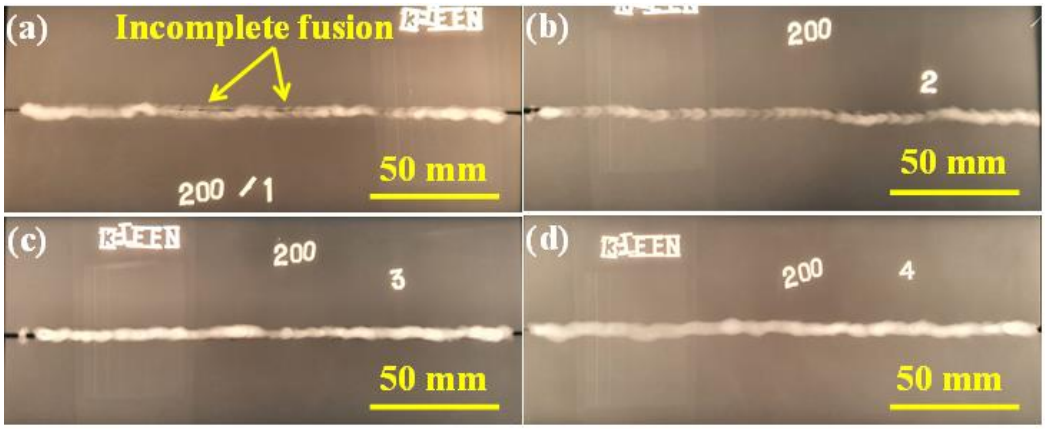

Fig. 4 The X-Ray radiography examination for stainless steels 304 and 304L welded joints at (a) ER309 and 70 A (b) ER309 and 80 A (c) ER304 and 70 A (d) ER304 and 80 A

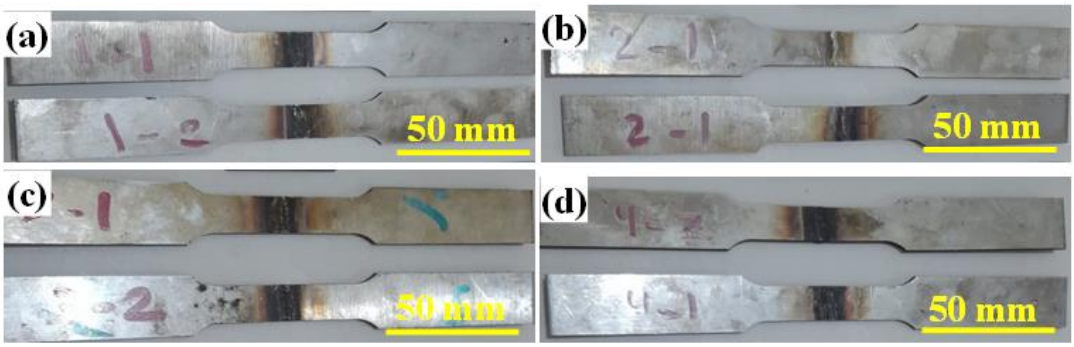

Fig. 5 The wire cut tensile test specimens for stainless steels 304 and 304L welded joints at (a) ER309 and 70 A (b) ER309 and 80 A (c) ER304 and 70 A (d) ER304 and 80 A

Table 5 Tensile properties of the base metals

Material	Yield Strength (MPa)	Ultimate strength (MPa)	Elongation (%)
stainless steels 304	265	650	55
stainless steels 304 L	310	620	40

Figure 6 shows the results of the transverse tensile tests conducted on the four TIG welding conditions with their respective standard deviation presented on the bar chart. Notably, increasing the welding current had a positive effect on the strength of the welds, regardless of the filler electrode type used [5]. For instance, when welding with ER309, the strength increased from 670 MPa to 677 MPa as the current was increased from 70 A to 80 A. Similarly, when welding with ER304, the strength increased from 689 MPa to 692 MPa due to the increase in current from 70 A to 80 A. These results indicate that higher welding currents can lead to stronger welds, which is an important consideration for applications that require high strength and durability. Moreover, it is worth noting that using ER304 as a filler electrode led to higher strength compared to using ER309 for both welding currents. For instance, the strength increased from 670 MPa to 689 MPa when switching from ER309 to ER304 when welding at 70 A, while the strength increased from 677 MPa to 692 MPa when using ER304 instead of ER309 when welding at 80 A. These findings suggest that ER304 is a more suitable filler electrode for achieving higher strength and improved mechanical properties in TIG welding of 304 and 304L stainless steels than ER309. The higher ultimate tensile strength (UTS) observed in the weld joints produced with ER304 filler electrode can be attributed to its higher UTS value compared to ER309. According to Table 3, the UTS of ER304 is 650 MPa, which is higher than the UTS of ER309 at 600 MPa. In conclusion, the highest transverse tensile strength was achieved by using 80 A as the welding current and ER304 as the filler electrode in this study. The higher heat input and faster cooling rate associated with welding with 80 results in a finer grain structure and more complete fusion in the weld metal, which led to the higher mechanical properties observed. In addition, the filler type and the welding speed have also a great effect of the archived mechanical properties. The measured UTS are in consistent with the presented [18].

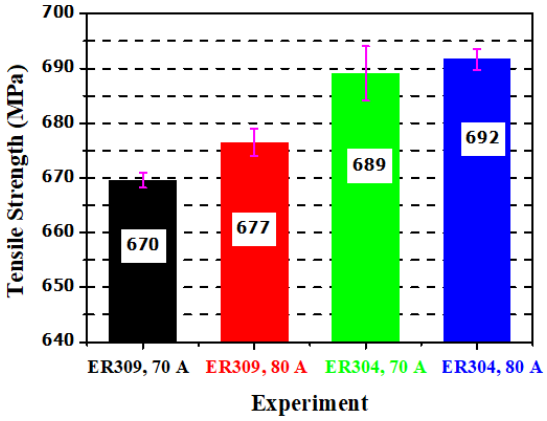

Fig. 6 The average UTS for the TIG welding joints at all the proposed welding condition.

The measured microhardness (HV) values for all the welded joints at all the proposed welding conditions at the BM, HAZ and WM are tabulated in **Table 6**. There is a variation in the measured microhardness values with the welding zones due to the microstructure variation resulting from the welding process.

Figure 7 displays the microhardness results obtained at different points within the BM, HAZ and WZ for TIG welded specimens under all welding conditions presented in **Table 4**. The microhardness variation from the BM to the WZ for the welded specimens is attributed to a microstructural change. For specimens welded with ER309 at 70 A and 80 A, the microhardness values within the HAZ were found to be higher than those of the WM, resulting in fractures within the WM, as illustrated in **Fig. 8 (a, b)**. Additionally, the microhardness values within the WZ were lower for experiment one (ER309, 70A) than for experiment two (ER309, 80A), which supports the tension test results presented in **Fig. 6**. Furthermore, for specimens welded with ER304 at 70 A an 80 A, the microhardness values within the HAZ were lower than those of the WM, leading to fractures within the HAZ for all tensile test specimens, as depicted in **Fig. 8 (c, d)**. These findings indicate that the microstructural changes in the HAZ significantly affect the mechanical properties of the welded specimens.

For specimens welded with ER309, the hardness of the HAZ is higher than that of the WZ, which means that the HAZ is more brittle and prone to cracking. This is because the ER309 filler metal has a higher carbon content than the BM, which increases the formation of martensite in the HAZ. The higher the welding current, the higher the hardness of the WZ, as more filler metal is deposited and more heat is generated. This is consistent with the tensile test results shown in Fig. 6, where the specimens welded with ER309 at 80 A had a higher ultimate tensile strength than those welded at 70 A. our results are in a good agreement with [19].

For specimens welded with ER304, the hardness of the HAZ is lower than that of the WZ, which means that the HAZ is more ductile and less likely to crack. This is because the ER304 filler metal has a lower carbon content than the BM, which reduces the formation of martensite in the HAZ.

Figure 9 shows that the optical microstructure of the BM of stainless steel 304. It is mainly austenite with a small amount of δ ferrite. The black striped structure is a skeletal δ ferrite, and the white matrix is austenite. In addition, stainless steel 304L has a very similar microstructure to stainless steel 304 (austenitic microstructure).

Table 6 Microhardness results at all the proposed welding conditions

Zone	Distance from the weld centre (mm)	Welding Condition			
		ER309, 70 A	ER309, 80 A	ER304, 70 A	ER309, 80 A
		Microhardness (HV)			
BM	-7	180	191	170	172
	-6	186	200	183	165
	-5	182	202	171	168
HAZ	-4	187	239	188	180
	-3	184	246	213	187
	-2	194	238	198	190
WZ	-1	174	218	233	187
	0	178	206	243	197
	1	175	216	212	181
HAZ	2	192	228	196	190
	3	185	225	203	209
	4	188	223	207	192
BM	5	197	217	189	185
	6	195	222	204	175
	7	198	210	200	188

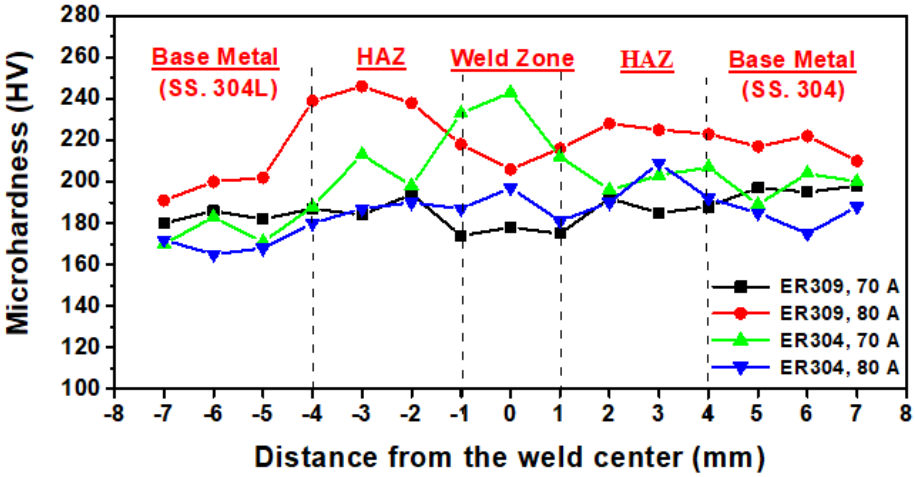

Fig. 7 Microhardness results for the welded joints between stainless steels 304 and 304L at different welding conditions through the BM, HAZ, and WM

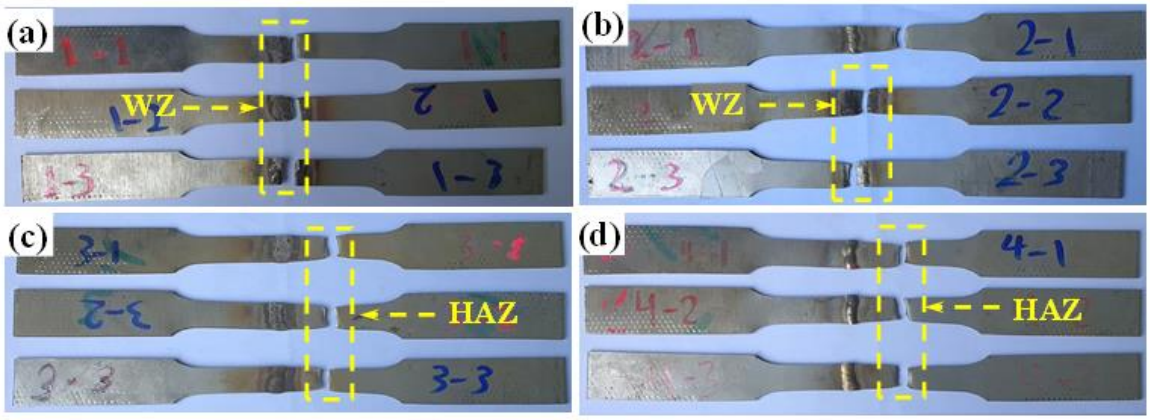

Fig. 8 Fractured tensile test specimens for stainless steels 304 and 304L welded joints at (a) ER309 and 70 A (b) ER309 and 80 A (c) ER304 and 70 A (d) ER304 and 80 A

To investigate the welding processes, metallographic analyses were conducted on the cross-sectional area of the welding specimens **Fig. 10** displays the optical microstructure of the welded specimens using ER309 at 70 A within the WZ and HAZ. In **Fig. 10 (a)**, the microstructure at the WZ and HAZ is depicted, revealing a coarse grain structure within the HAZ due to the heat accumulation during welding. **Fig. 10 (b)** shows a dark dendrite structure with austenitic and skeletal (vermicular) ferrite within the welding zone, with the dark areas representing ferrite and white areas representing austenite. Furthermore, **Fig. 10 (c)** presents a magnified photo of the HAZ, indicating that the WZ has a fine grain structure of smaller size compared to the BM's larger grain structure, which suggests a fine rearrangement of grains in the WZ.

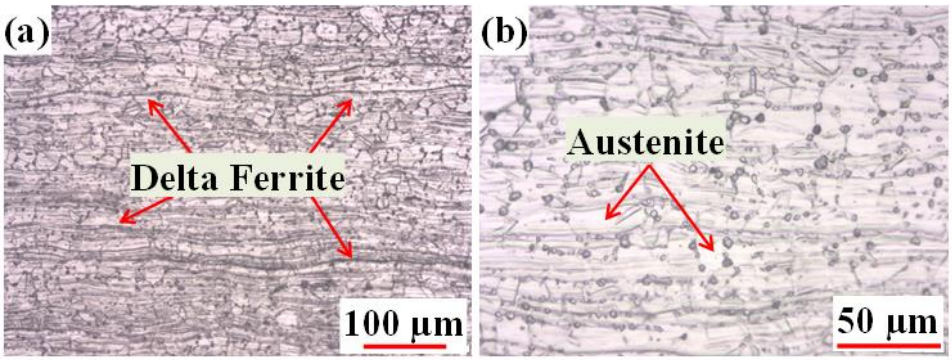

Fig. 9 Optical microstructure of stainless steels 304 at **(a)** Low magnification, **(b)** High magnification

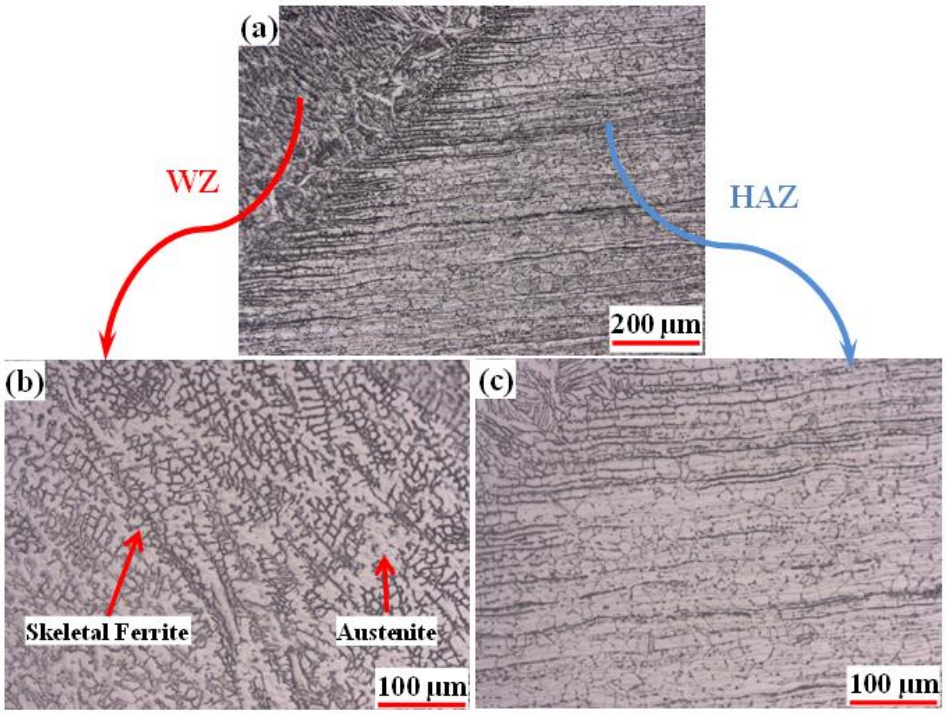

Fig. 10 Microstructure of the welded stainless steels 304 with 304L by ER309 and 70 A **(a)** WZ and HAZ **(b)** Magnified WZ **(c)** Magnified HAZ

Figure 11 displays the optical microstructure within the WZ for the four different welding experiments. **Fig. 11 (a, b)** represent the welding microstructure for welding experiments (one and two) being welded by ER309 at 70 A and 80 A, respectively. These figures reveal that the WZ consists of a dendritic microstructure from skeletal ferrite. The main difference between the two figures is that the dendrites become finer as the welding current increases, which is consistent with the tensile results presented in **Fig. 6**. Skeletal ferrite is a microstructure that consists of thin, plate-like grains of ferrite that form at lower cooling rates. This microstructure is less desirable in TIG stainless steel welds because it can reduce the toughness and ductility of the material.

On the other hand, **Fig. 11 (c, d)** show the welding microstructure for welding with ER304 at 70 A and 80 A, respectively. It is worth noting that the microstructure is nearly similar, which explains the small variation in the tensile test results between them. The microstructure is acicular ferrite, which is a microstructure that consists of fine needle-shaped grains of ferrite that form at high cooling rates. The acicular ferrite has a high aspect ratio, meaning that its length is much greater than its width. This microstructure is desirable in stainless steel welds because it provides good toughness and resistance to brittle fracture. The observed microstructure is in good agreement with the tensile test results presented in **Fig. 6**.

Weldability is an important parameter of the welding process, reflecting the metal's ability to be welded. The weldability of a metal can be inferred from the mechanical properties of its welded joints. In our study, we found that welding with a higher current (80 A) resulted in higher weldability than welding with a lower current (70 A). We also found that the type of filler material used can have a significant impact on weldability. For example, welding with ER304 resulted in higher mechanical properties than welding with ER309. Additionally, the carbon content of the base metal can also affect weldability [14]. Lower carbon content, such as in stainless steel 304L, leads to higher weldability than higher carbon content, such as in stainless steel 304.

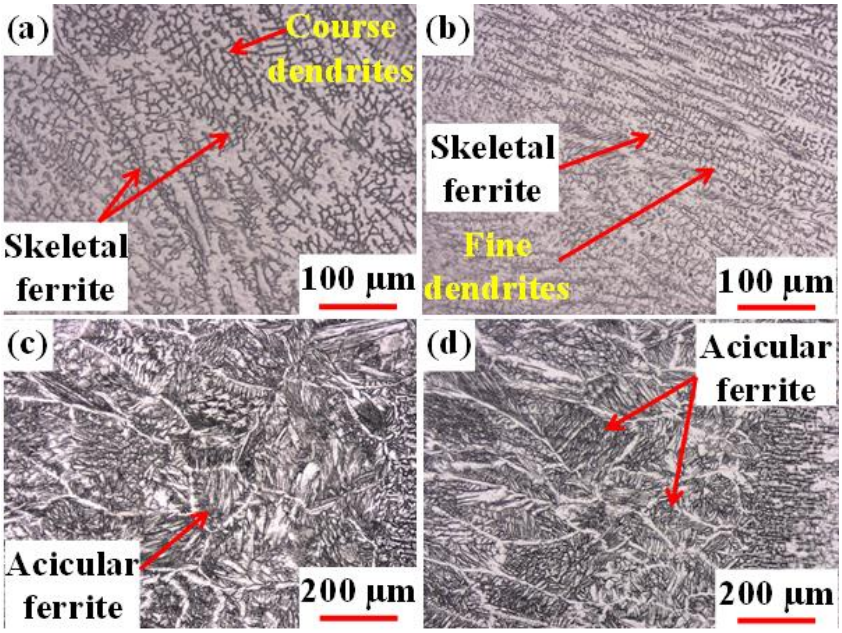

Fig. 11 Optical microstructure foe the WZ for **(a)** ER309, 70 A **(b)** ER309, 80 A **(c)** ER304, 70 A **(d)** ER304, 80 A.

CONCLUSION

- The use of ER304 electrode resulted in higher values for the average UTS (689 MPa, 692 MPa), regardless of the current used.
- Regardless of the electrode type, an increase in the applied current from 70 A to 80 A resulted in an increase in the average UTS (from 670 Mpa to 677 MPa for ER304 and from 689 MPa to 692 MPa for ER304).
- The strength of the weld joint was increased with both higher current and the use of ER304 filler.
- For all experiments except number one, the microhardness values of the welded specimens at the WZ and HAZ were greater than that of the BM due to the heat accumulation.
- The WZ was observed to have a fine-grained structure, while the BM had a comparatively coarser grain structure.
- A dendritic structure consisting of austenitic and skeletal ferrite was observed within the WZ for the experiments done with ER309.
- Austenitic microstructure with acicular ferrite was observed for the welding experiment being welded by ER304.

4. References

[1] ÇALIGÜLÜ U, CALIGULU U, DIKBAS H, TASKIN M (2012) Microstructural characteristic of dissimilar welded components (AISI 430 ferritic-AISI 304 austenitic stainless steels) by CO2 laser beam welding (LBW). Gazi University Journal of Science 25:35–51

[2] Di Schino A (2020) Manufacturing and applications of stainless steels. Metals (Basel) 10:327

[3] Maleque MA, Salit MS (2013) Materials selection and design. Springer

[4] Allgood LE (2011) Gas Tungsten Arc Welding

[5] Ogundimu EO, Akinlabi ET, Erinosho MF (2019) Effect of welding current on mechanical properties and microstructure of tig welding of type-304 austenite stainless steel. In: Journal of Physics: Conference Series. IOP Publishing, p 032022

[6] Yang Q, Xu W, Xiao Y, et al (2022) Microstructures and Mechanical Properties of 304 Stainless Steel Joints by Focused Ultrasound-Assisted TIG Welding. Metallography, Microstructure, and Analysis 11:141–149

[7] Saha M (2020) Effect of welding parameter of welded joint of stainless steel 304 by TIG welding. Available at SSRN 3643709

[8] Li D, Lu S, Dong W, et al (2012) Study of the law between the weld pool shape variations with the welding parameters under two TIG processes. J Mater Process Technol 212:128–136

[9] Kumari M, Barma JD, Singh S (2021) Parametric observation of TIG welding on AISI 304 stainless steel of thickness 5 mm. In: AIP Conference Proceedings. AIP Publishing

[10] Setyowati VA, Widodo EWR (2017) The Effect of TIG Welding for 304 and 304L Stainless Steel to Mechanical Properties, XRD and EDX Characterization as Pressure Vessel Materials. Jurnal Teknik Mesin 7:74–80

[11] Kurt Hİ, Samur R (2013) Study on microstructure, tensile test and hardness 304 stainless steel jointed by TIG welding. International Journal of Science and Technology 2:163–168

[12] Ugla AA (2018) Enhancement of weld quality of AISI 304L austenitic stainless steel using a direct current pulsed TIG arc. In: IOP Conference Series: Materials Science and Engineering. IOP Publishing, p 012075

[13] Kumar SR, Kumaran SS, Arravind MS, Venkateswarlu D (2019) Effect of microstructure and mechanical properties of austenitic stainless steel 1.6 mm butt welded by plasma arc welding. In: Materials Science Forum. Trans Tech Publ, pp 619–624

[14] El-Bitar T, El-Meligy M, Gamil M (2022) METALLURGICAL AND MECHANICAL INVESTIGATION OF TIG ARC WELDMENTS FOR API X60 STEEL PIPES. Acta Metallurgica Slovaca 28:19–24. https://doi.org/10.36547/ams.28.1.1324

[15] ASTM E (2001) Standard test methods for tension testing of metallic materials. Annual book of ASTM standards ASTM

[16] ASTM E (2006) 92: 2003: Standard Test Method for Vickers Hardness of Metallic Materials. ASTM International

[17] Standard A (2012) E407-07: Standard Practice for Microetching Metals and Alloys. ASTM International, West Conshohocken, PA 1–21

[18] Navaneethakrishnan N, Loganathan VN Welding Characteristics of 304, 306, 316 Stainless Steel: A Technical

[19] Kumar P, Sinha AN, Hirwani CK, et al (2021) Effect of welding current in TIG welding 304L steel on temperature distribution, microstructure and mechanical properties. Journal of the Brazilian Society of Mechanical Sciences and Engineering 43:369